Path Planning of Multi-UAS Communication Relay by Decentralized MPC

Fabio Augusto de Alcantara Andrade[1,3,4], Christopher Dahlin Rodin[1,2], Anthony Reinier Hovenburg[1,2], Tor Arne Johansen[1], Rune Storvold[3]

***Abstract*—When using Autonomous Surface Vehicles (ASV) in marine operations, long distances and/or low power transmissions may severely limit the communication between the ASV and the ground station. One solution to overcome this obstacle is to use a group of small Unmanned Aerial Systems (UAS) to act as relay nodes, in order to provide a user-defined minimum communication capability. To achieve this, we propose a decentralized cooperative multi-agent system using fixed-wing UAS with nonlinear model predictive control, which aims to guarantee a desired signal strength between the ASV and the ground station. The novelty of the presented research resides in the inclusion of the aircraft performance model and the effects of wind, together with the inclusion of the directivity of the antennas. Experimental results of the proposed method are obtained through simulations.**

I. Introduction

Utilizing an Autonomous Surface Vehicle (ASV) in maritime missions brings forth the need for a reliable communication link with sufficient signal strength between the ASV and the ground station. Although in some cases a direct link can be used, it is often severely limited in range and affected by the local geography. Satellite communication can manage longer distances, but can not always be used due to partial satellite coverage, limited bandwidth or the high associated costs. An alternative solution is to use autonomous fixed wing Unmanned Aerial Systems (UAS) to act as communication relay nodes in order to establish a communication link between the ASV and the ground station. By strategically coordinating the UAS' trajectories, the obtainable communication link can reach the desired signal strength over a larger distance.

In recent scientific literature, there are several approaches to solving similar problems. Grancharova et al. [1] used multiple rotary wing UAS to form a communication network between a base station, a stationary target and a moving target. The author used RF Signal Propagation, Loss, And Terrain (SPLAT!) for calculating the communication path losses. The path losses were approximated to linear functions, and a Model Predictive Control problem was solved by quadratic programming. Johansen et al. [2] describes the use of one fixed wing UAS as a communication relay node between a ground station and an Autonomous Underwater Vehicle (AUV), where the AUV was positioned at the ocean surface. In this work, horizontally omni-directional antennas were used. However, in their experiment, due to the vertical directionality of the antenna beam, the roll angle of the UAS affects the communication. Kim et al. [3] used multiple autonomous fixed wing UAS as communication relay nodes for a fleet of vessels using a decision making algorithm to choose the waypoints which could satisfy Dubins trajectories and lead to a configuration where the range between the nodes will be less than a specified minimum communication range. The solution was improved in [4], where the paths of the UAS were optimized using Nonlinear Model Predictive Control (NMPC), and the network connectivity was modelled in the context of Mobile Ad hoc NETworks (MANETs) based on global message connectivity. Here, the change on the directivity of the antenna pattern due to the effect of the attitude of the UAS was not considered. This made it simpler to model the communication characteristics, but also made it less realistic. In addition the method does not consider the effects of wind or the power consumption of the UAS. Braga et al. [5] optimized the communication Quality of Service, considering the power consumption and the bandwidth. Here, a simplified power consumption estimation was used, and, again, the wind and the UAS attitude effect on the radiation pattern were not considered. In recent studies, Palma et al. [6] performed field experiments using a UAS as a data mule, i.e. it was used to download and offload data sequentially, rather than to uphold a data link. Different protocols were tested where it is shown that the quality of the communication depends on the protocol being used. The author also states that the combination between the altitude and loiter radius, which determines the angle between the nodes, has a significant effect on the efficiency of data transfer due to the antenna-radiation patterns. Therefore, it is fundamental to define flight trajectories whilst taking this into consideration.

Dixon and Frew [7] used a decentralized algorithm based on the gradient of Signal-to-Noise Ratio (SNR) measurements to obtain a cascaded communication chain between a control station and a moving vehicle. A drawback of their method is the limitation in the vehicle dynamics – a cyclic motion is required in order to obtain an estimate of the SNR – which can result in a non-optimal path. The authors do not consider power consumption of the vehicles, resulting in a functional communication relay, but with a reduced duration compared to an algorithm that considers

[1]NTNU Centre for Autonomous Marine Operations and System, Department of Engineering Cybernetics, Norwegian University of Science and Technology, Trondheim, Norway

[2]Maritime Robotics A/S, Trondheim, Norway

[3]NORUT Northern Research Institute, Tromsø, Norway

[4]CEFET/RJ Federal Center of Technological Education of Rio de Janeiro, Rio de Janeiro, Brazil

the power consumption, and has more freedom in vehicle dynamics. Frew and Brown [8] considered a meshed network of UAV relay nodes. Experimental data showed that the meshed network improved the range and throughput of the communication link compared to a static meshed network.

This paper proposes a solution by using a decentralized nonlinear MPC to optimize the state of multiple UAS to achieve the desired signal strength between the ground station and the ASV. This is done while minimizing the power consumption of the maneuvering aircraft in order to maximize the mission endurance. As the directivity of the antennas is also considered, roll angles of the UAS are taken into account when determining the signal strength. The proposed solution also takes into account the effects of wind on the aircraft performance.

II. Methodology

A. Path Planning

Assuming that the path planning problem will start with all the UAS organized on a network topology (Fig. 1) providing the required transmitter-receiver signal strength between the ASV and the ground station, the aim of the algorithm is to optimize the states of the UAS to sustain a signal strength which does not fall below a preset requirement. A Nonlinear Model Predictive Control (NMPC) [9] method is used to optimize the velocity and bank angle of the UAS to achieve the desired signal strength while minimizing power consumption.

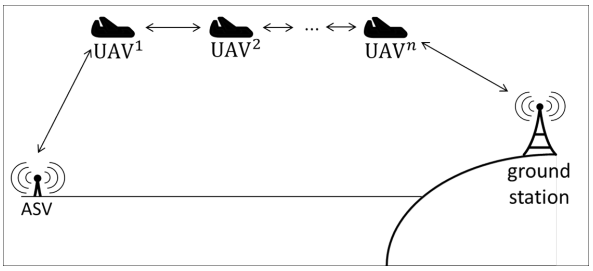

Fig. 1. Network topology

A centralized control system needs to optimize the control inputs of all the relay nodes, causing significantly increased complexity. With an increased number of relay nodes the method ultimately becomes unfeasible. Therefore, a fully decentralized NMPC is proposed, where each UAS plans its own path and attitude, taking into consideration the planned states of the other UAS and the planned position of the ASV in time. This can only be achieved under the assumption that the information can be shared between the UAS. Here the UAS only needs to be able to communicate with the adjacent nodes.

Assuming that the UAS will fly at a constant altitude maintained by the autopilot, a two-dimensional kinematics model can be used based on the Coordinated Flight Vehicle model [10] as:

$$\begin{pmatrix} \dot{x} \\ \dot{y} \\ \dot{\psi} \\ \dot{v_a} \\ \dot{\phi} \end{pmatrix} = f(\mathbf{x}, \mathbf{u}) = \begin{pmatrix} v_a \cos\psi + v_w \cos\psi_w \\ v_a \sin\psi + v_w \sin\psi_w \\ \frac{g \tan\phi}{v_g} \\ u_v \\ u_\phi \end{pmatrix} \quad (1)$$

where $\mathbf{x} = (x, y, \psi, v_a, \phi)$ are the North and East positions in the NED frame, heading, air-relative velocity (airspeed) and bank angle of the UAS, respectively. v_w and ψ_w are the velocity and heading of the wind, v_g is the ground-relative velocity, or ground speed, and g is the gravity acceleration. $\mathbf{u} = (u_v, u_\phi)$ are the acceleration control input and the roll rate control input, respectively.

The model is discretized by the forward Euler method:

$$\mathbf{x}_{k+1} = f_d(\mathbf{x}_k, \mathbf{u}_k) = \mathbf{x}_k + T_s f(\mathbf{x}_k, \mathbf{u}_k) \quad (2)$$

where T_s is the sampling period.

The overall control problem is decomposed as a unique local control problem for each UAS node, where each UAS optimizes its own state based on the signal strength with respect to its two adjacent nodes, while taking into consideration the planned states of the adjacent nodes. Collision avoidance and power consumption are also considered.

Considering n UAS ($\mathbf{x}^i, \forall i \in \{1, ..., n\}$), a fixed ground station ($\mathbf{x}^0$) and a moving ASV ($\mathbf{x}^{n+1}$), the NMPC algorithm finds a control input sequence $U_k^i = \{\mathbf{u}_0^i, \mathbf{u}_1^i, ..., \mathbf{u}_{N-1}^i\} \in R^{2\times N}$ for the ith UAS, which solves the following optimal control problem:

$$\text{minimize} \quad \delta^i(\bar{\mathbf{x}}_N^i) + \sum_{k=0}^{N-1} L^i(\bar{\mathbf{x}}_k^i, \mathbf{u}_k^i) \quad (3)$$

$$\text{subject to} \quad \mathbf{x}_{k+1}^i = f_d(\mathbf{x}_k^i, \mathbf{u}_k^i) \quad (4)$$

$$v_{a_{min}} \le v_{ak}^i \le v_{a_{max}} \quad (5)$$

$$\phi_{min} \le \phi_k^i \le \phi_{max} \quad (6)$$

$$\dot{v}_{a_{min}} \le u_{vk}^i \le \dot{v}_{a_{max}} \quad (7)$$

$$\dot{\phi}_{min} \le u_{\phi k}^i \le \dot{\phi}_{max} \quad (8)$$

$$|\mathbf{C}_1(\mathbf{x}_k^i - \mathbf{x}_k^j)| > r_c, \forall j \in \{1, ..., n\} \backslash \{i\} \quad (9)$$

where

$$\delta^i(\bar{\mathbf{x}}_N^i) = aJ^i(\bar{\mathbf{x}}_N^i) \quad (10)$$

$$L^i(\bar{\mathbf{x}}_k^i) = aJ^i(\bar{\mathbf{x}}_k^i) + b{u_{vk}^i}^2 + c{u_{\phi k}^i}^2 \quad (11)$$

and

$$J^i(\bar{\mathbf{x}}_k^i) = \alpha E^i(\mathbf{C}_2\bar{\mathbf{x}}_k^i) + (1-\alpha)P^i(\mathbf{C}_3\mathbf{x}_k^i) \quad (12)$$

$\bar{\mathbf{x}}_k^i = [\mathbf{x}_k^{i-1}, \mathbf{x}_k^i, \mathbf{x}_k^{i+1}]$ are the states of the adjacent nodes, N is the number of horizon steps and r_c is the minimum safe distance between the UAS to avoid collision. a, b, c are constant weighting factors and $\mathbf{C}_1$, $\mathbf{C}_2$ and $\mathbf{C}_3 \in R^{2\times 5}$ are used to define which state variables of the vehicles are to be considered in the equations. In case of $\mathbf{C}_1$, only the x and y

positions should be used, in case of $\mathbf{C}_2$, x, y, ψ and ϕ are used and in case of $\mathbf{C}_3$, only v_a and ϕ are used.

$$\mathbf{C}_1 = \begin{bmatrix} 1 & 0 & 0 & 0 & 0 \\ 0 & 1 & 0 & 0 & 0 \end{bmatrix} \tag{13}$$

$$\mathbf{C}_2 = \begin{bmatrix} 1 & 0 & 0 & 0 & 0 \\ 0 & 1 & 0 & 0 & 0 \\ 0 & 0 & 1 & 0 & 0 \\ 0 & 0 & 0 & 0 & 1 \end{bmatrix} \tag{14}$$

$$\mathbf{C}_3 = \begin{bmatrix} 0 & 0 & 0 & 1 & 0 \\ 0 & 0 & 0 & 0 & 1 \end{bmatrix} \tag{15}$$

As the main goal of the system is to provide the desired signal strength with the lowest power consumption, $E^i(\mathbf{C}_2\bar{\mathbf{x}}^i)$ through Eq. (16) is the difference between the desired and actual signal strength between the ith UAS and its adjacent nodes, while $P^i(\mathbf{C}_3\mathbf{x}^i)$ through Eq. (27) is the power consumption function. Finally, α is a weighting factor that defines how much power can be used to improve the communication.

B. Signal strength

The function of the transmitter-receiver signal strength between the ith UAS and its adjacent nodes is the sum of the difference between the calculated signal strength and the desired signal strength, for the ith UAS and each of the two adjacent nodes. If the signal strength is equal or higher than the desired one, the error is considered to be zero.

$$E^i(\mathbf{C}_2\bar{\mathbf{x}}^i) = \Delta Err^i(\mathbf{C}_2\bar{\mathbf{x}}^i)\frac{\frac{\pi}{2} - \arctan(-\beta\Delta Err^i(\mathbf{C}_2\bar{\mathbf{x}}^i))}{\pi} \tag{16}$$

where β is the constant which defines how close the curve will be to a conditional function and $\Delta Err^i(\bar{\mathbf{x}}^i)$ is the difference between the desired signal strength and the minimum calculated signal strength as the following:

$$\Delta Err^i(\mathbf{C}_2\bar{\mathbf{x}}^i) = P_d - P^i_{min}(\mathbf{C}_2\bar{\mathbf{x}}^i) \tag{17}$$

where P_d is the desired signal strength and $P^i_{min}(\mathbf{C}_2\bar{\mathbf{x}}^i)$ is the lowest signal strength between the ith UAS and each one of its adjacent nodes, as the lowest signal strength is the one limiting the link. To calculate the minimum value between two elements, the following equation is used:

$$\begin{aligned} &P^i_{min}(\mathbf{C}_2\bar{\mathbf{x}}^i) = \\ &0.5(P^{i-1}_{dBm}(\mathbf{C}_2\mathbf{x}^{i-1}, \mathbf{C}_2\mathbf{x}^i) + P^i_{dBm}(\mathbf{C}_2\mathbf{x}^i, \mathbf{C}_2\mathbf{x}^{i+1}) - \\ &\sqrt{(P^{i-1}_{dBm}(\mathbf{C}_2\mathbf{x}^{i-1}, \mathbf{C}_2\mathbf{x}^i) - P^i_{dBm}(\mathbf{C}_2\mathbf{x}^i, \mathbf{C}_2\mathbf{x}^{i+1}))^2)} \end{aligned} \tag{18}$$

where $P^i_{dBm}(\mathbf{C}_2\mathbf{x}^i, \mathbf{C}_2\mathbf{x}^{i+1}) = 10\log P^i(\mathbf{C}_2\mathbf{x}^i, \mathbf{C}_2\mathbf{x}^{i+1}) + 30$.

To calculate the signal strength between nodes, the Friis equation [11] is used to calculate the received power, based on the distance between the nodes and the directivity of the antennas:

$$\begin{aligned} P^i(\mathbf{C}_2\mathbf{x}^i, \mathbf{C}_2\mathbf{x}^{i+1}) = \; & P_t \cdot D^{i,i+1}(\mathbf{C}_2\mathbf{x}^i, \mathbf{C}_1\mathbf{x}^{i+1}) \cdot \\ & D^{i+1,i}(\mathbf{C}_2\mathbf{x}^{i+1}, \mathbf{C}_1\mathbf{x}^i) \cdot \\ & FSPL(\mathbf{C}_1\mathbf{x}^i, \mathbf{C}_1\mathbf{x}^{i+1}) \end{aligned} \tag{19}$$

where $FSPL(\mathbf{C}_1\mathbf{x}^i, \mathbf{C}_1\mathbf{x}^{i+1})$ is the Free-Space-Path-Loss:

$$FSPL(\mathbf{C}_1\mathbf{x}^i, \mathbf{C}_1\mathbf{x}^{i+1}) = (\frac{\lambda}{4\pi d^i(\mathbf{C}_1\mathbf{x}^i, \mathbf{C}_1\mathbf{x}^{i+1})})^2 \tag{20}$$

and P_t is the transmitted power, λ is the wavelength, $D^{i,i+1}(\mathbf{x}^i, \mathbf{x}^{i+1})$ is the directivity gain with respect to the position and antenna angle of the ith and $(i+1)$th nodes, and $d^i(\mathbf{C}_1\mathbf{x}^i, \mathbf{C}_1\mathbf{x}^{i+1})$ is the distance between nodes:

$$\begin{aligned} &d^i(\mathbf{C}_1\mathbf{x}^i, \mathbf{C}_1\mathbf{x}^{i+1}) = \\ &\sqrt{(x^i - x^{i+1})^2 + (y^i - y^{i+1})^2 + (z^i - z^{i+1})^2} \end{aligned} \tag{21}$$

where z^i is the constant z offsets of the antennas of the ith node.

The directivities are obtained by the following equation:

$$D^{i,i+1}(\mathbf{C}_2\mathbf{x}^i, \mathbf{C}_1\mathbf{x}^{i+1}) = 4\pi\frac{F(\theta(\mathbf{C}_2\mathbf{x}^i, \mathbf{C}_1\mathbf{x}^{i+1}))}{F_{avg}} \tag{22}$$

where $F(\theta(\mathbf{C}_2\mathbf{x}^i, \mathbf{C}_1\mathbf{x}^{i+1}))$ is the power radiation pattern of the antenna and F_{avg} is the average power density over a sphere, given by:

$$F_{avg} = \int_0^{2\pi}\int_0^{\pi} F(\theta(\mathbf{C}_2\mathbf{x}^i, \mathbf{C}_1\mathbf{x}^{i+1}))sin\theta d\theta d\gamma \tag{23}$$

where $\theta(\mathbf{C}_2\mathbf{x}^i, \mathbf{C}_1\mathbf{x}^{i+1})$ is the angle between the antenna of the ith node and the body of the $(i+1)$th node:

$$\theta(\mathbf{C}_2\mathbf{x}^i, \mathbf{C}_1\mathbf{x}^{i+1}) = \arcsin\frac{\mathbf{R}_z(\psi^i)\mathbf{R}_x(\phi^i)\mathbf{v}(\mathbf{C}_1\mathbf{x}^{i+1} - \mathbf{C}_1\mathbf{x}^i)}{d^i(\mathbf{C}_1\mathbf{x}^i, \mathbf{C}_1\mathbf{x}^{i+1})} \tag{24}$$

where $\mathbf{v} = [0\ 0\ 1]$ is the reference vector from where the angle θ will be calculated relative to, $\mathbf{R}_x(\phi)$ and $\mathbf{R}_z(\psi)$ are the rotation matrices in x and y with respect to the angles ϕ and ψ [12].

$$\mathbf{R}_x(\phi) = \begin{bmatrix} 1 & 0 & 0 \\ 0 & cos\phi & -sin\phi \\ 0 & sin\phi & cos\phi \end{bmatrix} \tag{25}$$

$$\mathbf{R}_z(\psi) = \begin{bmatrix} cos\psi & -sin\psi & 0 \\ sin\psi & cos\psi & 0 \\ 0 & 0 & 1 \end{bmatrix} \tag{26}$$

C. Aircraft power consumption

To obtain an accurate model of the overall system performance, the in-flight performance of the aircraft needs to be considered [13][14]. In this study both the aircraft's airspeed and bank angle are being optimized. Therefore it is necessary for the aircraft performance model to evaluate the in-flight power consumption, and express the penalty for changing airspeed and performing longitudinal maneuvering. For a

propeller-driven aircraft in steady flight the consumed power (P) is found through:

$$P = \frac{D\, v_a}{\eta_p} \tag{27}$$

Where D is the aerodynamic drag force experienced by the aircraft, v_a is the airspeed, and η_p is the total propulsion efficiency. For level flight the generated lift L equals the aircraft weight W. However, when the bank angle ϕ is no longer zero, the lift force is rotated by an angle ϕ in relation to the gravity component. This results in:

$$L \cos\phi = W \tag{28}$$

In this study the loss of lift caused by an increased bank angle is mitigated by increasing the airspeed. This is done so that a constant altitude can be maintained. It is therefore necessary to account for the effects of bank angle ϕ on the required airspeed v_a. When considering a coordinated flight the adjusted airspeed for a turn with constant-C_L is found through:

$$v_a = \sqrt{\frac{2W}{\rho_\infty S}\frac{n}{C_L}} = v_\infty \sqrt{n} \tag{29}$$

Here v_∞ is the required airspeed for level unaccelerated flight in meter per second. S is the aircraft's effective wing surface in square meter, W is the aircraft's total weight in Newton, and ρ_∞ is the air density in kilogram per cubic meter. The initial aerodynamic lift coefficient C_L is determined through:

$$C_L = \frac{2W}{\rho_\infty S v_\infty^2} \tag{30}$$

Furthermore, n is the load-factor, which in accelerated flight is larger than zero. This is defined as:

$$n = \frac{1}{\cos\phi} = \left(\frac{T}{W}\right)\left(\frac{L}{D}\right) \tag{31}$$

In level unaccelerated flight and constant speed level turns the condition applies that the generated thrust force T equals the drag force experienced by the aircraft. Assuming a general simplified drag model in a coordinated flight where trim drag is neglected, and the thrust line is parallel to the airspeed, the drag force D is obtained through [15]:

$$D = T = \frac{1}{2}\rho_\infty v_a^2 S \left[C_{D_0} + k\left(\frac{nW}{qS}\right)^2\right] \tag{32}$$

Here C_{D_0} is the aircraft's zero-lift drag coefficient. Finally, k is the lift-induced drag constant, which is defined as:

$$k = \frac{1}{\pi\ AR\ e} \tag{33}$$

Here AR is the aircraft's effective aspect ratio, and e is the Oswald efficiency factor.

Fig. 2. Skywalker X8 sUAS - operated by AMOS UAVLab

In this study the Skywalker X8 aircraft is used in the simulations. The X8 (Fig. 2) is a small battery-powered unmanned aircraft in flying-wing configuration. It has a wingspan of 2.1 meters with a mission-ready weight of 3.36 kilograms. The effective wing surface is approximately 0.74 square meters. Two elevon control surfaces are located on the outer wings to provide longitudinal, lateral and directional control of the aircraft. The aerodynamic lift model that was used in the simulation was based on wind tunnel experiments, which are described in the submitted work in [16], while the value for k is assumed to be 0.0907. The propulsion characteristics are unknown to the authors. Therefore for the remainder of this study the propulsion efficiency η_p is assumed to be invariable at 0.5, and the maximum thrust T_{max} is assumed to be constant at 25 Newtons with ideal-battery discharge characteristics.

From Eq. (31) and (32) it can be observed that as the bank angle increases, the power consumption increases. The in-flight performance, and consequently the power consumption, are affected through the required increase in airspeed. It is important to note that to avoid the aircraft from entering a stall, the maximum load factor n_{max} is limited by the available thrust. The thrust-limited maximum load factor can be found by substituting the maximum available thrust in Eq. (31). Solving for ϕ yields the thrust-limited maximum bank angle. The minimum value for the airspeed v_{stall} as a function of load factor n and $C_{L_{max}}$ can be found by inserting the maximum lift coefficient into Eq. 29. This results in:

$$v_{stall} = \sqrt{\frac{2}{\rho_\infty}\frac{W}{S}\frac{n}{C_{L_{max}}}} \tag{34}$$

Finally, a *structural* limitation exists. As the structural limit load factor for the Skywalker X8 platform is not known to the authors it is chosen to implement a stricter limitation for the simulations as further referenced in Section IV.

III. System description

The simplified block diagram of the control system is shown in Figure 4. The Model Predictive Control (MPC) runs inside DUNE [17], which is an open source robot framework developed by the Underwater Systems and Technology

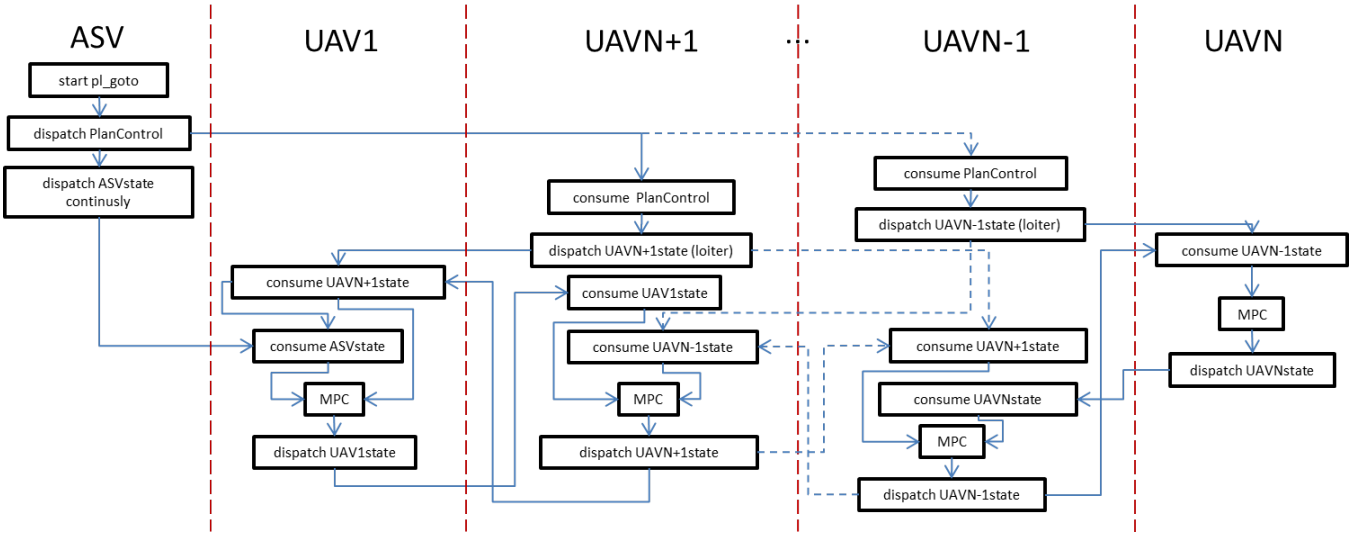

Fig. 3. Communication between nodes using IMC messages and DUNE Tasks

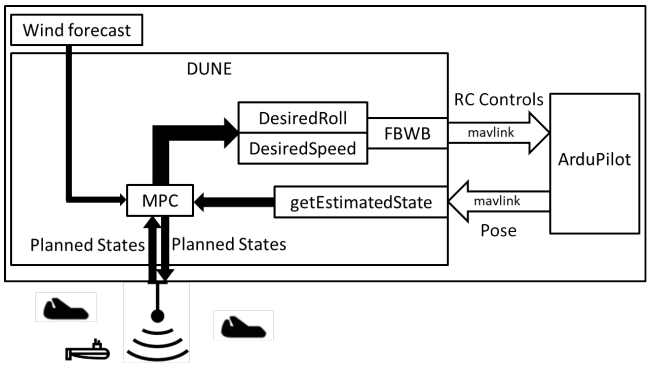

Fig. 4. Individual system's block diagram

Laboratory (LSTS) of the University of Porto. DUNE is installed on the onboard computer and communicates with the ArduPilot board via Micro Air Vehicle Communication Protocol (MAVLink). When executing the maneuver, the ArduPilot opperates in Fly-By-Wire-B (FBWB) mode and gets the desired roll and airspeed as Radio Control (RC) inputs from DUNE.

The MPC is included in a DUNE task. Every time the UAS gets the updated planned states of the adjacent nodes, it calls the MPC function and, based on its current state and on the adjacent nodes states, it calculates its own planned states. In this step, the wind forecast present in a data file is also considered. After the optimization, the UAS broadcasts its planned states to the other nodes and sends the commands to the ArduPilot.

The coordination of the mission is done by the dispatch and consumption of Inter-Module Communication Protocol (IMC) messages. In DUNE, if a IMC message is dispatched by a node, all nodes that are monitoring that type of message will receive it and run the routine binded to the reception of that message.

A. Mission coordination

Each UAS awaits the start of the mission in loiter mode. When the ASV starts the plan, it dispatches a "PlanControl" message that is consumed by the UAS. All UAS then start the maneuver and dispatch their planned states considering the loiter maneuver, except the UAS closest to the ASV and the one closest to the Ground Station. These two UAS wait for the planned states of their adjacent nodes and are the first ones to run the MPC. Figure 3 shows the flow chart of the IMC messages between the nodes.

IV. Simulations

The first simulation (fig. 5) was done for a scenario considering two UAS to close the wi-fi link between the ASV and a ground station. The simulation starts when the ASV is at position [300,300] - 423 meters away from the ground station. The first UAS starts the mission at position [100,100] and the second one at position [200,200]. The ASV is moving north with constant speed over ground of 1.6 m/s.

It is possible to notice that when the mission starts, the straight link between the ASV and the ground station has less than -70 dBm, which was chosen as the desired signal strength as it is the minimum power to establish a wi-fi connection. Using the UAS, the ASV can progress with the mission for more 8 minutes, when UAS are not capable to provide the desired signal strength anymore. This means an increase of 8 minutes to the operation, and this can also be expanded if more UAS are used as relay nodes.

Considering the different limitations of the load factor, the maximum bank angle ϕ_{max} is chosen to be restricted to 20^o, which offers an associated stall speed of 8.9 meter per second. Therefore the minimum airspeed $v_{a_{min}}$ is defined to be 12.0 meters per second. The other parameters used in the simulation are shown in tables I, II and III.

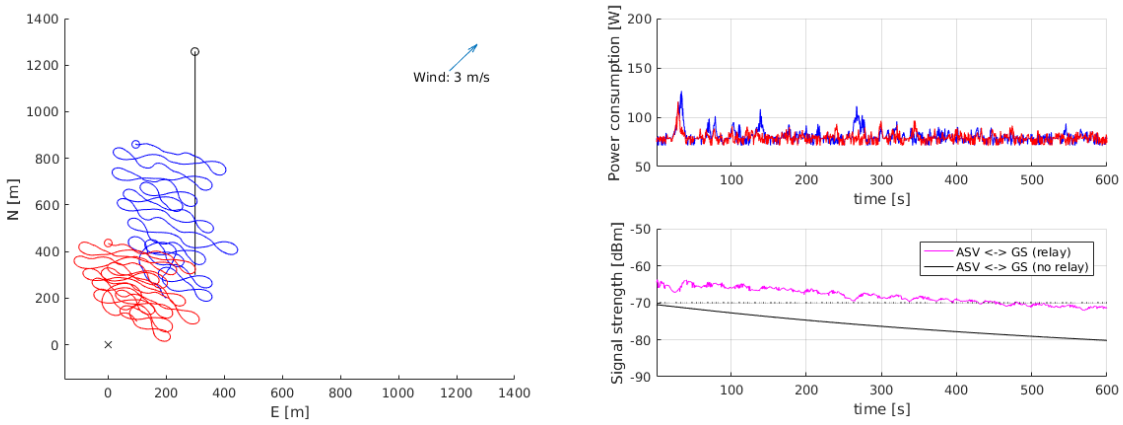

Fig. 5. First simulation scenario. Ground station as a black x, ASV's path in black, UAS 1's path in blue and UAS 2 path's in red.

To solve the NMPC problem, Particle Swarm Optimization (PSO) [18] was used. The algorithm was developed using CUDA C programming language, benefiting from the parallelization to reduce the computational time. Each optimization takes around 250 ms, proving the algorithm suitable for real-time applications. The computational time can be reduced if necessary, by adjusting the horizon and number of steps. This would result in a decrease of the optimality, but may be beneficial in real environments, as the system will calculate the control inputs for a state closer to the state that it was when the calculation began.

A second simulation was done for a scenario where the nodes were equipped with a communication system inspired by the characteristics of the Maritime Broadband Radio (MBR) 144 radio from the company Kongsberg Maritime [19], together with a 7 dBi antenna with around 25 degrees of $HPBW$ in the elevation plane. This radio can provide up to 20 km of range [20] for a frequency between 4.90 and 5.85 GHz. The communication parameters of this simulation were chosen as it is shown in table IV and the results are shown in fig. 6. The ASV starts the simulation at position [13500,13500] (around 19 km from the ground station) and the UAS 1 and UAS 2 at [4500,4500] and [8000,8000] respectively. Here the duration of the mission was set to be one hour. It was found that besides the significant increase in obtainable communication range, it is also noticeable that the link between the ASV and the ground station when using the UAS as relay nodes has a higher signal strength throughout the duration of the mission.

V. Discussion and Future Work

In the current implementation of the algorithm, the wind is assumed to be constant. For small a aircraft, however, the wind can have a major effect on the power consumption. It would therefore be beneficial to use a wind map in the optimization algorithm. A proposed method is to fit an analytic function to a discrete wind map in order to use it in the MPC.

TABLE I
MPC Parameters

Param	Name	Value	Unit
v_w	velocity of wind	3.0	m/s
ψ_w	heading of wind	0.7	rad
g	gravity acceleration	9.81	m/s^2
t	time horizon	15.0	s
N	horizon steps	30	m/s
h	altitude of UAS	100.0	m
hN	altitude of the ground station	20	m
$v_{a_{min}}$	minimum airspeed	12.0	m/s
$v_{a_{max}}$	maximum airspeed	20.0	m/s
ϕ_{min}	minimum bank angle	-0.349	rad
ϕ_{max}	maximum bank angle	0.349	rad
$\dot{v}_{a_{min}}$	minimum acceleration	-0.2	m/s^2
$\dot{v}_{a_{max}}$	maximum acceleration	0.2	m/s^2
$\dot{\phi}_{min}$	minimum bank angle rate	-1.4	rad/s
$\dot{\phi}_{max}$	maximum bank angle rate	1.4	rad/s
r_c	safe distance between UAVs	50.0	m
a	weight of cost function	1.0	
b	weight of acceleration control	1.0	
c	weight of bank angle rate control	1.0	
α	weight of signal strength / power saving	0.99	

TABLE II
Communication Parameters of Scenario 1

Param	Name	Value	Unit
β	conditional function fitting constant	99999	
P_d	desired signal strength	-70	dBm
P_t	transmitter power	100.0	mW
λ	wavelength	12.5	cm
$HPBW$	Half-Power-Bandwidth	2.09	rad

TABLE III
Power Consumption Parameters

Param	Name	Value	Unit
η_p	propulsion efficiency	0.5	
W	aircraft weight	32.96	N
ρ_∞	air density	1.225	kg/m^3
C_{D_0}	zero-lift drag coefficient	0.125	
k	lift-induced drag constant	0.0224	
S	wing surface	0.74	m

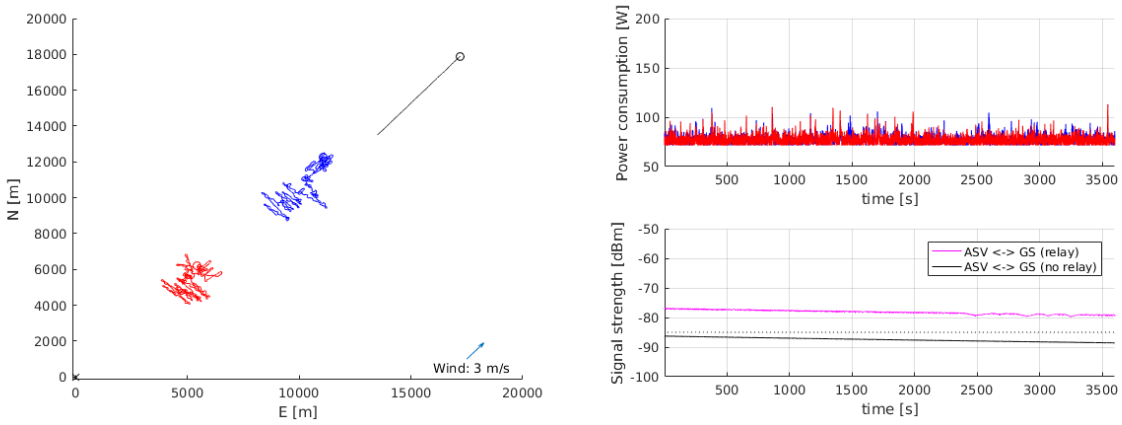

Fig. 6. Second simulation scenario. Ground station as a black x, ASV's path in black, UAS 1's path in blue and UAS 2 path's in red.

TABLE IV
COMMUNICATION PARAMETERS OF SCENARIO 2

Param	Name	Value	Unit
β	conditional function fitting constant	99999	
P_d	desired signal strength	-85	dBm
P_t	transmitter power	2.0	W
λ	wavelength	6.0	cm
$HPBW$	Half-Power-Bandwidth	0.437	rad

Field experiments are also planned in order to define constraints for the signal strength variations, that could affect the overall network capability.

Regarding the number of UAS and the ASV behavior, it is necessary to simulate scenarios where more UAS are used and that the ASV moves in different patterns to evaluate the system performance. Simulations using different altitudes for the UAS should also be considered.

VI. CONCLUSION

In this paper, a communication relay solution was presented. The goal of the system is to provide a minimum signal strength between the Autonomous Surface Vehicle and a ground station by using Unmanned Aerial Systems as communication relay nodes. The system was build to be used with DUNE robotic framework and was modeled as a Nonlinear Model Predictive Control problem. Simulations show that the system is capable to be tested in field experiments and may be a suitable tool in maritime missions.

ACKNOWLEDGEMENT

The authors want to thank Kristoffer Gryte at NTNU Centre for Autonomous Marine Operations and Systems (AMOS) for supplying the aerodynamic model of the aircraft that was used in this study.

This work has been carried out at the Centre for Autonomous Marine Operations and Systems (AMOS), supported by the Research Council of Norway through the Centres of Excellence funding scheme, project number 223254. This project has received funding from the European Union's Horizon 2020 research and innovation programme under the Marie Sklodowska-Curie grant agreement No 642153.

REFERENCES

[1] A. Grancharova, E. I. Grøtli, D.-T. Ho, and T. A. Johansen, "Uavs trajectory planning by distributed mpc under radio communication path loss constraints," *Journal of Intelligent & Robotic Systems*, vol. 79, no. 1, p. 115, 2015.

[2] T. A. Johansen, A. Zolich, T. Hansen, and A. J. Sørensen, "Unmanned aerial vehicle as communication relay for autonomous underwater vehiclefield tests," in *Globecom Workshops (GC Wkshps), 2014*. IEEE, 2014, pp. 1469–1474.

[3] S. Kim, P. Silson, A. Tsourdos, and M. Shanmugavel, "Dubins path planning of multiple unmanned airborne vehicles for communication relay," *Proceedings of the Institution of Mechanical Engineers, Part G: Journal of Aerospace Engineering*, vol. 225, no. 1, pp. 12–25, 2011.

[4] S. Kim, H. Oh, J. Suk, and A. Tsourdos, "Coordinated trajectory planning for efficient communication relay using multiple uavs," *Control Engineering Practice*, vol. 29, pp. 42–49, 2014.

[5] J. Braga, R. Praveen Jain, A. Pedro Aguiar, and J. Sousa, "Self-triggered time coordinated deployment strategy for multiple relay uavs to work as a point-to-point communication bridge," in *Research, Education and Development of Unmanned Aerial Systems (RED-UAS), 2017 Workshop on*. IEEE, 2017, pp. 0–0.

[6] D. Palma, A. Zolich, Y. Jiang, and T. A. Johansen, "Unmanned aerial vehicles as data mules: An experimental assessment," *IEEE Access*, 2017.

[7] C. Dixon and E. W. Frew, "Maintaining optimal communication chains in robotic sensor networks using mobility control," *Mobile Networks and Applications*, vol. 14, no. 3, pp. 281–291, 2009.

[8] E. W. Frew and T. X. Brown, "Networking issues for small unmanned aircraft systems," *Journal of Intelligent and Robotic Systems*, vol. 54, no. 1-3, pp. 21–37, 2009.

[9] E. F. Camacho and C. B. Alba, *Model predictive control*. Springer Science & Business Media, 2013.

[10] A. Rucco, A. P. Aguiar, F. L. Pereira, and J. B. de Sousa, "A predictive path-following approach for fixed-wing unmanned aerial vehicles in presence of wind disturbances," in *Robot 2015: Second Iberian Robotics Conference*. Springer, 2016, pp. 623–634.

[11] J. D. Kraus and R. J. Marhefka, "Antennas for all applications," *Antennas for all applications, by Kraus, John Daniel; Marhefka, Ronald J. New York: McGraw-Hill, c2002.*, 2002.

[12] R. W. Beard and T. W. McLain, *Small unmanned aircraft: Theory and practice*. Princeton university press, 2012.

[13] S. Gudmundsson, "A biomimetic, energy-harvesting, obstacle-avoiding, path-planning algorithm for uavs," Ph.D. dissertation, Embry-Riddle Aeronautical University, 2016.

[14] S. Gudmundsson, V. Golubev, S. Drakunov, and C. Reinholtz, "Biomimetic opportunistic approaches in energy-conserving/harvesting flight-path modeling for uas," *AIAA Modeling and Simulation Technologies Conference*, 2016.

[15] J. Anderson, *Aircraft performance and design*, ser. McGraw-Hill international editions: Aerospace science/technology series. WCB/McGraw-Hill, 1999.

[16] K. Gryte, R. Hann, A. Mushfiqul, J. Roh, T. A. Johansen, and T. I. Fossen, "Aerodynamic modeling of the skywalker x8 fixed-wing unmanned aerial vehicle," *Submitted to 2018 International Conference on Unmanned Aircraft Systems (ICUAS)*, 2018.

[17] J. Pinto, P. S. Dias, R. Martins, J. Fortuna, E. Marques, and J. Sousa, "The lsts toolchain for networked vehicle systems," in *OCEANS-Bergen, 2013 MTS/IEEE*. IEEE, 2013, pp. 1–9.

[18] R. Eberhart and J. Kennedy, "A new optimizer using particle swarm theory," in *Micro Machine and Human Science, 1995. MHS'95., Proceedings of the Sixth International Symposium on*. IEEE, 1995, pp. 39–43.

[19] *Maritime Broadband Radio - MBR*, (accessed March 23, 2018). [Online]. Available: https://www.km.kongsberg.com/ks/web/nokbg0240.nsf/AllWeb/BCCBAC3EA4EA6785C1257E280039BD63

[20] A. Zolich, A. Sœgrov, E. Vågsholm, V. Hovstein, and T. A. Johansen, "Coordinated maritime missions of unmanned vehiclesnetwork architecture and performance analysis," in *Communications (ICC), 2017 IEEE International Conference on*. IEEE, 2017, pp. 1–7.